

Ultrasonication-Assisted Fabrication of High-Performance Carbon Nanotube Composites

Xuebing Zhang^{1,2}, Shuxuan Qu², Wengang Yang², Han Zhang³, and Weibang Lyu^{2*}

¹ School of Nano-Tech and Nano-Bionics, University of Science and Technology of China, Hefei, China,

² Innovation Center for Advanced Nanocomposites, Suzhou Institute of Nano-Tech and Nano-Bionics, Chinese Academy of Sciences, Suzhou, China,

³ School of Engineering and Materials Science, Queen Mary University of London, London, UK

* Corresponding author (wblv2013@sinano.ac.cn)

Keywords: Ultrasonication, Carbon nanotube composites, Bundle, Orientation, Chemical modification

ABSTRACT

Carbon nanotubes (CNTs) are considered ideal reinforcement for the next generation of lightweight and high-strength composites due to their superior mechanical, electrical and thermal properties. However, due to the extremely high specific surface area, CNTs tended to aggregate into bundles under the action of inter-tube van der Waals force, resulting in that the mechanical properties of CNT composites were much lower than expected. Based on this, this work focused on the CNTs' bundle of composites. In the process of resin infiltration, ultrasonication was introduced and the bundles' diameter was regulated by cavitation effect. In addition, the ultrasonic cavitation was improved and optimized to assist mechanical stretching and chemical modification to maximumly enhance the CNT orientation and load transfers of CNT composites, and finally realized the preparation of high-performance CNT composites (strength and modulus were up to 3.2 GPa and 204 GPa). The influence trends and mechanism of ultrasonic cavitation on the structure and properties of CNT and its composites were systematically studied.

1 INTRODUCTION

As a nanofiber material, Carbon nanotubes (CNTs) have higher specific strength and specific modulus than traditional high-performance fibers (such as carbon fiber and glass fiber), as well as excellent electrical and thermal properties [1]. Therefore, researchers believed that CNT would be an ideal reinforcement in a new generation of lightweight and high-strength composites [2]. Accordingly, compared with traditional fiber reinforced composites, CNT composites have not only structural advantages, but also functional advantages [3].

According to Coleman's study [4], the strength and modulus of CNT composites were positively correlated to CNT content, CNT orientation, and CNT/matrix interfacial load transfers. Extensive studies have found that infiltrating resin into macroscopic assemblies of CNTs could fabricate composites with high CNT content. The alignment of CNTs within composites could be enhanced through stretching prior to curing. Meanwhile, some efforts have also been devoted to improve the interfacial load transfer efficiency by means of chemically modifying. For example, Chen prepared CNT film by CVD method, and then infiltrated epoxy resin solution into CNT network under pressure to prepare composite with CNT mass fraction of 59% and tensile strength of 1.4 GPa [5]. Jolowsky successfully increased the ultimate stretching ratio of CNT/BMI composites to 80% by controlling the ambient temperature during the stretching process. Under the optimal process conditions, the strength and modulus of oriented composites reached 1.58GPa and 252 GPa [6]. Park proposed a method of chemical cross-linking between CNTs through diazo salt reaction to improve the load transfer efficiency between CNTs, giving CNT fibers the tensile strength (3.7 N/tex) comparable to that of the strongest carbon fiber (Toray T1100 carbon fiber) [7].

It can be found that researchers in this field have made great efforts in the above three aspects under the inspiration of the traditional short-fiber composite strengthening theory. However, it is still

impossible to achieve a breakthrough in the performance of CNT composites, which may be related to the structural characteristics of CNT. Different from traditional short fiber reinforced composites (such as short carbon fiber reinforced composites), the reinforcement phases in CNT composites are mostly in the form of bundles rather than monodisperse CNTs, because CNTs have extremely high specific surface area and are easily clustered into bundles under the action of inter-tube van der Waals (vdWs) forces. Because of the dense structure of the bundle, the resin molecules can't penetrate into the bundle structure, limiting the distribution of resin uniformity. When the CNT composite is subjected to an external load, only the CNT on the outer part of the bundle bears the load while the CNT on the inner part does not. In this case of bundled CNTs, the interfacial load transfer ability of the composites can't be further improved, which is one of the fundamental reasons for the failure of mechanical properties of CNT composites. Therefore, reducing the diameter of CNT bundle is another new challenge to improve the performance of CNT composites.

Based on the above discussion, this work explored the influence of ultrasonication on the diameter of CNT bundles in CNT films and their composites, and developed the technology of regulating the diameter of bundle by ultrasonic cavitation, which improved the load transfer ability and mechanical properties of CNT composites. Subsequently, ultrasonic cavitation was introduced into mechanical stretching and chemical modification to maximumly enhance the CNT orientation and load transfers of CNT composites, and the preparation of ultra-high strength CNT composites (strength and modulus were up to 3.2 GPa and 204 GPa, respectively) was realized. The influence trends and mechanism of ultrasonic cavitation on the structure and properties of CNT and its composites were systematically studied.

2 EXPERIMENTS AND METHODS

2.1 Ultrasonication-assisted resin infiltration

Epoxy resin was diluted in the solvent (acetone) and the mass fraction of resin in the solution was set as 15%. CNT films of 6 cm × 6 cm size were then immersed in the epoxy resin solution at room temperature. The home-made ultrasonication setup was used to assist resin infiltration. A series of sonication time (i.e. 0, 4, 8, and 16 min) and sonication power (i.e. 36, 72, and 108 W) were adopted to reveal their effects on the structures and properties of CNT composites. After infiltration process, the resin impregnated CNT films (CNT prepreps) were placed in a vacuum oven at 50°C for 0.5 h to remove the solvent, and then sandwiched between two layers of ventilated felt and peel ply under 20 MPa pressure and 75°C for 1 h to remove the excess resin from the interior of CNT films (pre-gluing treatment). Finally, CNT prepreps were cured through hot pressing under 20 MPa pressure, following the curing cycle of 90°C for 1 h, 120°C for 2 h, and 150°C for 3 h.

2.2 Ultrasonication-assisted mechanical stretching

Firstly, a rectangular CNT film (40 cm×1 cm) was immersed in 40 wt% epoxy/acetone solution and ultrasonicated for 5 minutes (power density 0.1 W/cm³) to acquire CNT prepreps. Then, the CNT prepreps was stretched at a speed of approximately 1 mm/min via a home-made stretching device. During stretching process, the resin solution was ultrasonicated with different sonication power densities (i.e., 0.1, 0.15, and 0.2 W/cm³). All samples were stretched to their ultimate stretching ratio, as subjectively determined before any visible tearing would occur. Then, the oriented CNT prepreps were transformed into CNT composite after solvent removal treatment, pre-gluing and curing.

2.3 Ultrasonication-assisted chemical modification

Specific experimental steps were as follows: (1) 10 ml deionized water was mixed with 80 ml concentrated sulfuric acid under ice bath condition, then 1 g sodium nitrite and 0.6 g p-phenylenediamine were added carefully, and then placed the solution on a magnetic agitator for 2 h at 60 °C; (2) the CNT film was immersed in diazo salt solution at 60 °C, during which the ultrasonication was introduced to realize the ultrasound-assisted chemical modification process; (3) the modified CNT film was cleaned with deionized water and repeated until the pH value of the system rose to about 7.05, then the sample was placed in a vacuum drying oven for 1 h; (4) 3 g BMI resin was dissolved in 102.3 mL N-N dimethylformamide (DMF) solvent and stirred in a magnetic agitator for 2 h; (5) the modified

CNT film was immersed in BMI resin solution for 2 h to make the resin molecules fully infiltrated CNT film. Then, the oriented CNT prepreps were transformed into CNT composite after solvent removal treatment, pre-gluing and curing.

3 RESULTS AND DISCUSSION

3.1 Ultrasonication-assisted resin infiltration

3.1.1 Structure and morphology of CNT films and their composites

Fig. 1a₁-d₁ presented the SEM images of CNT films before and after ultrasonication in pure solvent. CNTs were mostly randomly aligned within all these films, and the films were of high porosity, making the resin infiltration possible. Fig. 1a₂-d₂ showed the histograms of CNT bundle diameter, and the statistical analysis found that the diameter of CNT bundles increased with sonication times, where it was about 21.6 nm in the untreated CNT film, while it increased to 24.5, 28.3 and 33.4 nm after ultrasonic treatment for 4, 8 and 16 min, respectively.

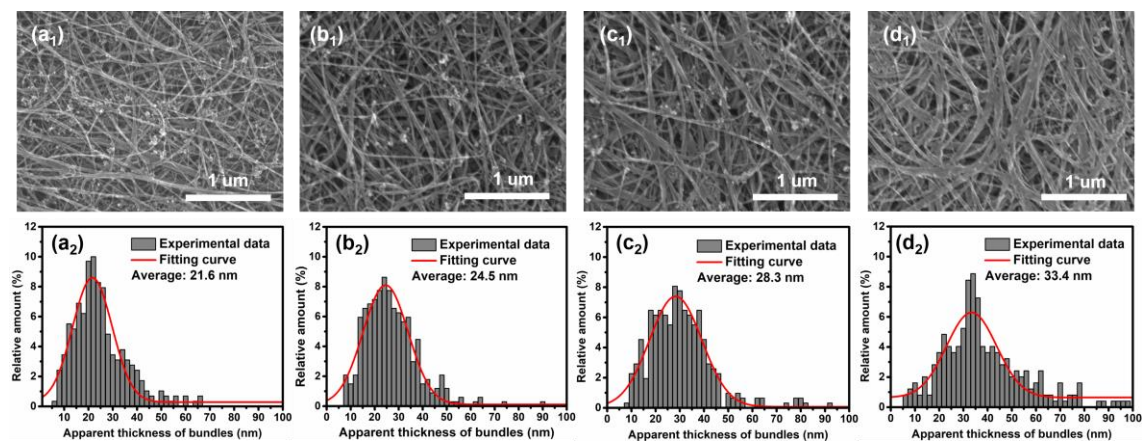


Fig. 1. (a₁-d₁) SEM images and (a₂-d₂) histograms of CNT bundles diameter of the CNT films after ultrasonic treatment in pure solvent for (a) 0, (b) 4, (c) 8 and (d) 16 min, respectively.

Fig. 2a showed the TEM image of a typical branched CNT bundles within a CNT film, where a 42 nm thick bundle split into two thinner branches of 16 and 26 nm thick. When the ultrasound waves propagate in the solution, the induced bubbles experience the process of formation, growth, and collapse, resulting in cavitation effect, and the instantaneous temperature and pressure induced by bubble collapse can be as high as 5000 K and 50 MPa, respectively [8]. The strong shock waves between the branches radiate to all directions and push the individual branches to further separate with each other when the impact force exceed the vdWs interaction between CNTs. This sonication induced de-bundling processing was schematically illustrated in Fig. 2b. As the cavitation bubbles continue to explode, large CNT bundles can be divided into smaller ones. However, when the sonication was stopped, these exfoliated small bundles would like to re-assemble into large bundles again under the inter-tube vdWs forces, thus resulting in thickened bundles. Fig. 2c schematically illustrated this de-bundling and re-bundling process.

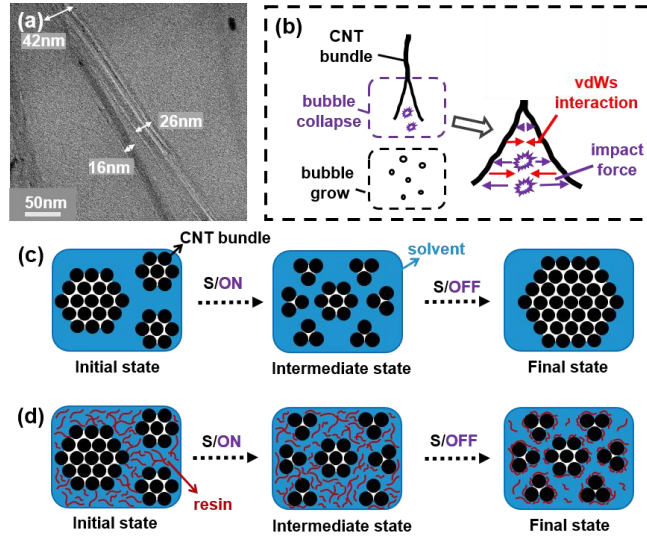


Fig. 2. (a) TEM image of branched CNT bundles, (b) schematic of the de-bundle processing, structural evolution of bundles in (c) pure solvent and (d) resin solutions.

Fig. 3a₁-d₁ show the SEM images of CNT prepregs before and after ultrasonication. For a better imaging of surface CNTs, CNT prepregs were washed by immersing them in acetone for 2 h to remove excessive resin materials from the prepregs surface. Specifically, for the samples without ultrasonication, the average diameter of CNT bundles was 61 nm, and some large bundles over 70 nm thick could be observed (Fig. 3a₁). After sonicated for 4, 8 and 16 min, the average diameter of CNT bundles decreased to about 59, 39 and 28 nm (Fig. 3b₁-d₁), respectively.

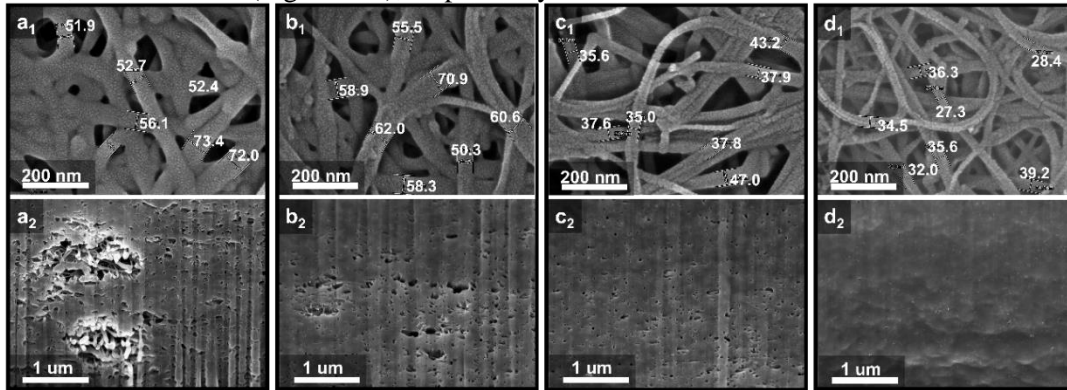


Fig. 3. (a₁-d₁) SEM images of the microscopic morphology of washed CNT prepregs, (a₂-d₂) Cross-section morphology of cured CNT composites, where a, b, c and d correspond to sonication time of 0, 4, 8 and 16 min, respectively.

Similar to the sonication of CNT films in pure solvent, it was also expected that during the sonication of CNT films in resin solution, large bundles separated into smaller ones when the energy provided by ultrasonication exceeded the vdWs cohesive energy between CNTs. The resin molecules then got into the enlarged inter-bundle areas and wrapped onto CNT surfaces (Fig. 2d), thus preventing the bundles from re-bundling after the sonication was stopped. This de-bundling process increased the interface area between CNTs and matrix and thus promoted the stress transfer efficiency in composites [9]. It was worth noting that the de-bundling effect was less obvious for a short sonication time (such as 4 min in the present study), as the provided sonication energy was not enough to overcome the vdWs cohesive energy between CNTs. When the sonication time increased to 8 or 16 min, the diameter of CNT bundles decreased dramatically, suggesting a stronger de-bundling effect.

To reveal the effect of ultrasonication on the resin distribution within CNT film-based composites, the cross-sections of these materials were characterized through SEM analyses (Fig. 3a₂-d₂). For composites without sonication treatment, enormous large voids can be found (Fig. 3a₂), indicating poor

resin infiltration. After sonicated for 4 min, large voids disappeared, while small voids still existed (Fig. 3b₂). The number and size of voids further decreased after sonicated for 8 min (Fig. 3c₂), and no visible voids could be found after sonicated for 16 min (Fig. 3d₂), indicating that the resin were almost thoroughly infiltrated into the voids in the CNT network.

3.1.2 Properties of CNT composites

Different sonication time and power were applied to investigate the effect of ultrasonication on the mechanical and electrical properties of CNT composites. The stress-strain curves and tensile mechanical properties are shown in Fig. 4a-c. The strength and modulus of the composites without ultrasonic treatment are 467 MPa and 10.9 GPa, respectively, which are over 2 times of pure CNT films. This indicated that the resin infiltration would effectively enhance the tensile mechanical properties of CNT films, which was in consist with previous studies [10]. By increasing the sonication time, the tensile mechanical properties of CNT composite films increased firstly and then decreased. After sonicated for 8 min, the tensile strength and modulus reached to the maximum of 583 MPa and 14.6 GPa, respectively, which were 24.8% and 33.9% higher than these of untreated ones. However, when further increasing the sonication time to 16 min, the strength and modulus of samples were reduced and even lower than those of untreated samples.

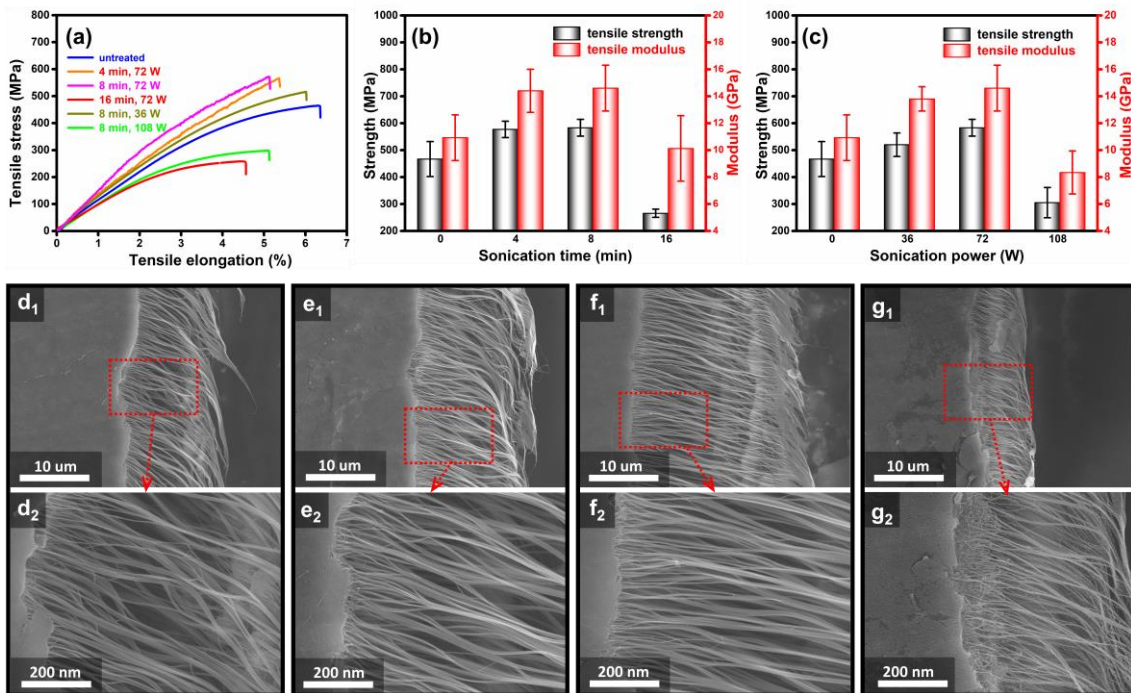


Fig. 4. (a) typical stress-strain curves, sonication (b) time and (c) power depend of the tensile mechanical properties, and low (d₁–g₁) and high (d₂–g₂) magnification SEM images of fractographies of CNT composites, where d, e f and g correspond to sonication time of 0, 4, 8 and 16 min, respectively.

To further reveal the structure dependence of the tensile properties of CNT composites, the fractographies of these composites were characterized through SEM analyses. As shown in Fig. 4d-g, CNT bundles were pulled out from the resin matrix in the fractured area. For the untreated composites, sparse and large diameter CNT bundles can be observed in the high magnification SEM image (Fig. 4d₂), resulted in limited reinforcing efficiency and undesirable mechanical properties. For the composites which sonicated for 4 min (Fig. 4e) and 8 min (Fig. 4f), CNT bundles which pulled out from the resin were thinner, which was in consist with the thinning trends indicated in Fig. 3a₁-d₁. In this respect, more CNTs could thus interact with resin materials and share the loading within these composites, leading to higher load transfer efficiency and mechanical properties [9]. As the sonication time was extended to 16 min, although CNT bundles were also thinner, their length was significantly shorter (Fig. 4g) due to excessive sonication energy.

The effect of sonication power on the mechanical properties of CNT composites were also

investigated and shown in Fig. 4c. For all these samples, the sonication time was set as 8 min. Similar to the dependence of sonication time, the tensile strength and modulus increased firstly and then decreased. In summary, with the increase of sonication energy, CNT bundles diameter decreased while the defects ratio of CNTs increased, which played positive and negative roles on the mechanical properties of CNT composites, respectively. The balance of these two effects is the key to obtain high-performance CNT composites.

3.2 Ultrasonication-assisted mechanical stretching

3.2.1 Stretchability of CNT preregs and the alignment of CNTs

During stretching process, different sonication power densities were selected to investigate their influence on the stretchability of CNT preregs. In this work, the ultimate stretching ratio was selected to quantitatively evaluate the stretchability of CNT preregs. The average results showed that the ultimate stretching ratio of CNT preregs without ultrasonication was 32.1%, and the stretchability of CNT preregs first increased and then decreased as the sonication power density increased (Fig. 5a). Specifically, the ultimate stretching ratios of CNT preregs were approximately 32.8%, 38.3% and 30.7%, corresponding to sonication power densities of 0.1, 0.15 and 0.2 W/cm^3 , respectively. The ultimate stretching ratio of CNT preregs under the optimal ultrasonic condition was increased by 19.3%, compared with those samples without ultrasonication.

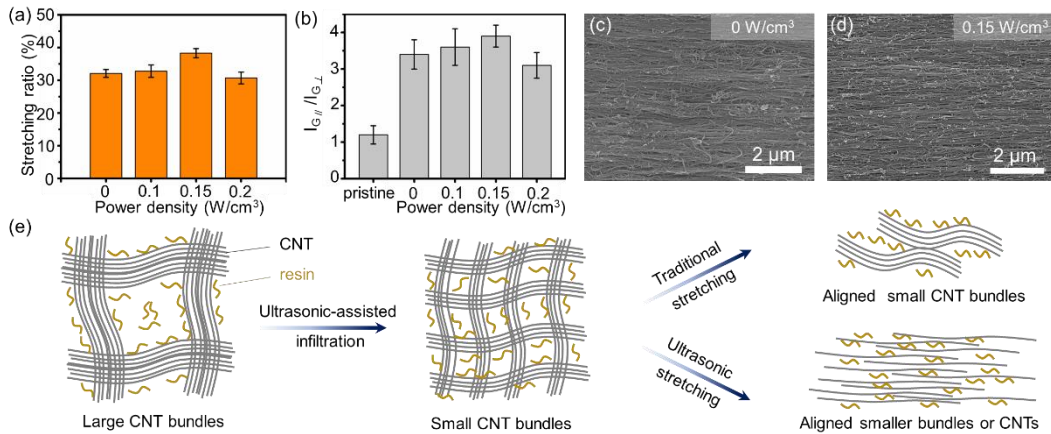


Fig. 5. (a) The ultimate stretching ratio and (b) the value $I_{G//}/I_{G\perp}$ of aligned CNT preregs treated with different sonication power densities. Surface morphology of aligned CNT preregs treated (c) without and (d) with ultrasonication (0.15 W/cm^3). (e) Schematic diagram of mechanism of ultrasonication on stretching process of CNT preregs.

Fig. 5c and d showed the surface morphology of CNT preregs stretched without and with ultrasonication (0.15 W/cm^3). Apparently, the introduction of ultrasonication during stretching process significantly increased the ultimate stretching ratio of CNT preregs, and simultaneously lead to the higher orientation and the lower waviness of CNT bundles. Quantitative evaluation of the CNTs alignment was conducted by polarized Raman spectroscopy and calculating $I_{G//}/I_{G\perp}$, where $I_{G//}$ and $I_{G\perp}$ represent the G-band intensities and were measured when the incident laser beam was in directions parallel and perpendicular to the orientation directions of the CNT nanocomposites [11]. The value $I_{G//}/I_{G\perp}$ for CNT preregs stretched without ultrasonication was 3.4 (Fig. 5b). Similar to the trend of stretchability of CNT preregs, the values $I_{G//}/I_{G\perp}$ first increased and then decreased with increasing sonication power density, which were 3.6, 3.9 and 3.1 for the 32.8%, 38.3% and 30.7% stretched CNT preregs, respectively.

The reasons for the above changing trend of stretchability of CNT preregs may be related to the following two aspects: On one hand, the de-bundling effect continuously separated large CNT bundles into smaller ones. Once transient ultra-high shock waves induced by ultrasonication exceed the vdWs forces between CNTs, and the bundles may be separated. Finally, the resin molecules diffused into the interior of the bundles under the drive of osmotic pressure and wrapped on the CNT surface [12], resulting in an increase of interface area within the composite. Therefore, the more CNTs wrapped with

the resin matrix in CNT prepregs, the more CNTs involved in relative slip motion, resulting in a higher ultimate stretching rate and alignment of CNT prepregs, as shown in Fig. 5e. On the other hand, overhigh sonication power density was unfavorable, such as 0.2 W/cm³, which excessively loosened the CNT prepregs and worsen the contact between adjacent CNTs, leading to a poor stretchability.

3.2.1 The properties of aligned CNT nanocomposites

Fig. 6a showed the typical stress–strain curves of the aligned CNT nanocomposites. With the increase of sonication power densities, the tensile strength of the aligned CNT nanocomposites increased first and then decreased. Particularly, as shown in Fig. 6b, the strength and modulus of aligned CNT nanocomposites treated with a sonication power density of 0.15 W/cm³ were the highest, 2.11 GPa and 104.7 GPa, which were 43.5% and 68.8% higher than those of aligned CNT nanocomposites without ultrasonication. The improvement of mechanical properties may be attributed to the following two aspects. On one hand, the de-bundling effect caused by ultrasonic cavitation and the sufficient infiltration of resin increased the interfacial area in CNT nanocomposites, leading to considerable load transfer [9]. On the other hand, ultrasonication improved the stretchability of CNT prepregs, making CNTs more aligned in the orientation direction. Furthermore, the fracture toughness of aligned CNT/epoxy films treated with a sonication power density of 0.15 W/cm³ was 45.6 J/cm², which was 42.5% higher than those of aligned CNT nanocomposites without ultrasonication (Fig. 6c).

However, the strength and modulus of CNT nanocomposites treated with 0.2 W/cm³ were worse than that of nanocomposites treated with lower sonication power densities. In addition to the low stretchability caused by the overhigh power density, it was also related to the severe damage to CNT caused by the cavitation effect. Previous studies have shown that ultrasonication would destroy the inherent structure of CNTs that were dispersed either in water or in other media [13, 14], which could inhibit the composites' properties.

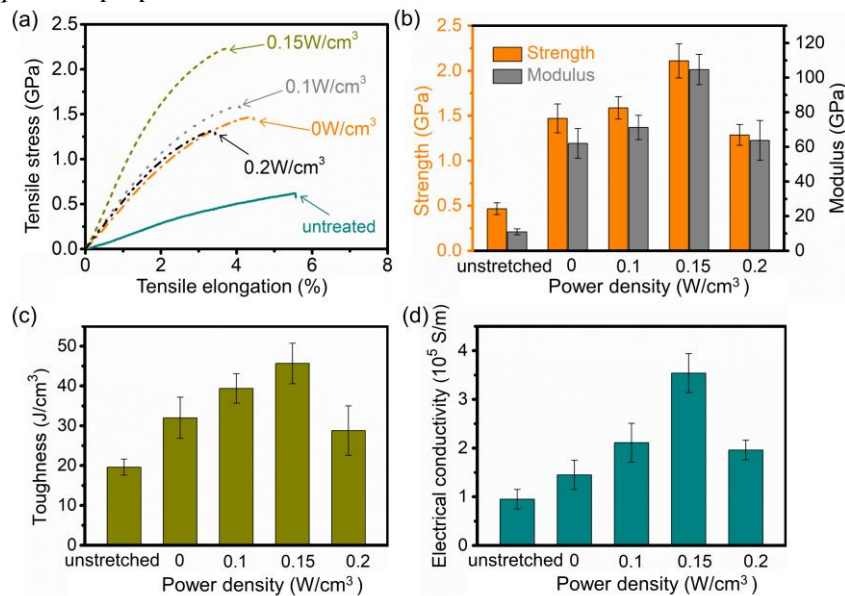


Fig. 6. (a) Typical stress-strain curves, (b) strength and modulus, (c) toughness and (d) electrical conductivity measurements paralleling to the orientation direction of CNT nanocomposites.

The electrical conductivity of the aligned CNT/epoxy nanocomposites was measured and summarized in Fig. 6d. Similar to the change trend of mechanical properties, the electrical conductivity of CNT nanocomposites also increased first and then decreased as the power density increased. For the untreated CNT nanocomposites, the electrical conductivity was 0.95×10^5 S/m. After stretching without ultrasonication, the conductivity of the aligned nanocomposite films increased to 1.45×10^5 S/m due to the improvement of CNT orientation. Moreover, under the ultrasonication conditions, the de-bundling degree and orientation of CNT nanocomposites were further improved, resulting in the increase of electrical conductivity to the maximum 3.54×10^5 S/m when the sonication power density reached 0.15 W/cm³, which was 144.1% higher than that of aligned samples without ultrasonication. Besides, the decrease in electrical conductivity when the power density was 0.2 W/cm³ was the result of a

combination of the CNT intrinsic bodies' damage and the poor CNT orientation caused by overhigh sonication power density.

3.3 Ultrasonication-assisted chemical modification

3.3.1 Chemical modification reaction mechanism of CNT films

The chemical modification process of CNT was divided into two stages, which were the stage of diazotization reaction and the stage of reaction of diazo salt with CNT. Fig. 7a and b showed the overall process of diazotization reaction. Firstly, sodium nitrite was decomposed into nitrite ion and sodium ion in sulfuric acid, in which nitrite ion was transformed into diazotization particles through hydrogenation, dehydration and other processes under acidic conditions (Fig. 7a). Secondly, the diazotized particles reacted with p-phenylenediamine and underwent a series of proton transfer processes, and finally dehydrated to form diazo salt (Fig. 7b).

Fig. 7c showed a schematic diagram of the reaction process between diazo salt and CNT. Although the optimal situation was that the amino groups at both ends of the p-phenylenediamine molecule were diazotized, and each diazo salt particle reacted with two CNTs to achieve cross-linking of CNTs. However, due to the uncontrollability of the experimental conditions and the uncertainty of the reaction, there were incomplete cross-linked CNT in the modified system, that was, only one end of the diazo salt particles successfully grafted CNT and the other end was not grafted CNT.

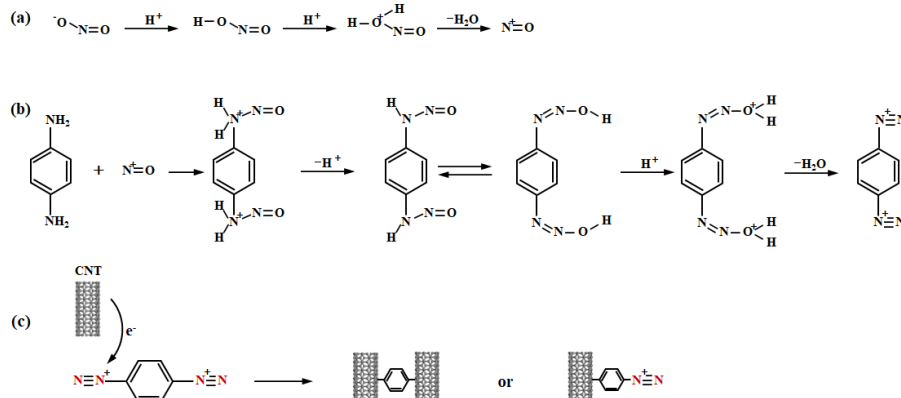


Fig. 7. (a) The formation process of diazotized particles, (b) the formation process of diazonium salts, (c) schematic diagram of modification reaction of CNT.

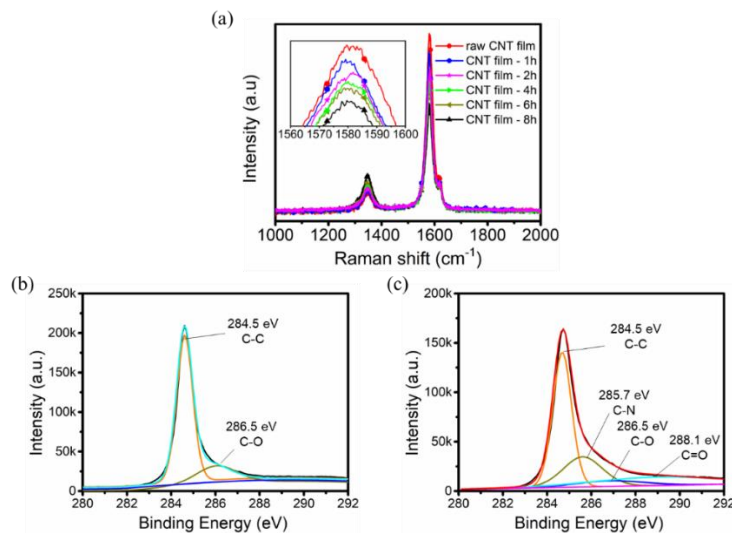


Fig. 8. Raman and XPS spectra of CNT films before and after modification. (a) Raman spectra of CNT film under different modified reaction time treatment conditions, (b) XPS spectra of original CNT film, (c) XPS spectra of modified CNT film.

In order to prove that small organic molecules were successfully grafted onto the surface of CNT,

the modified CNT films were characterized by Raman spectroscopy. As shown in Fig. 8a, the I_G/I_D value of the raw CNT film was 5.0. However, the I_G/I_D values of the modified CNT films decreased gradually with the increase of reaction time. When the reaction time reached 1, 2, 4, 6 and 8 h, the I_G/I_D values of the modified CNT films decreased to 4.9, 4.2, 3.6, 3.2 and 2.4, indicating that the modification reaction reduced the crystallinity of carbon atoms in CNT.

Fig. 8b and c showed the XPS characterization of CNT films before and after the modification reaction. As shown in Fig. 8b, the XPS curves of the raw CNT film had two characteristic peaks at the positions of 284.5eV and 286.5eV, corresponding to C-C and C-O bonds respectively, in which C-C peak was stronger and C-O peak was weaker, indicating that the chemical bond in the system was mainly C-C bond. The XPS curves of the CNT film after the modified reaction (reaction time was 4 h) had four characteristic peaks (Fig. 8c), which corresponded to C-C bond at 284.5eV, C-N bond at 285.7eV, C-O bond at 286.5eV and C=O bond at 288.1eV, respectively. Compared with the raw CNT film, C-N bond and C=O bond were newly added in the modified CNT film. Combined with the chemical reagents used in the reaction process, we could confirm that these two corresponded to the C-N in the diazo salt particles and the carboxyl group introduced after the oxidation of CNT by strong acid. The above experimental results showed that the small organic molecules (diazo salt) were successfully grafted onto the surface of CNT.

3.3.2 Mechanical and electrical properties of chemical modified CNT composites

As shown in Fig. 9a and b, the strength and modulus of unmodified CNT composites were 466 MPa and 9.9 GPa, respectively. When the modification reaction time reached 1, 2, 4, 6 and 8 h, the strength and modulus of the material were 486 MPa and 11.7 GPa, 565 MPa and 15.1 GPa, 680 MPa and 19.9 GPa, 469 MPa and 15.6 GPa, 290 MPa and 14.4 GPa, respectively. It could be seen that the mechanical properties of the modified CNT composite increased first and then decreased with the increase of reaction time. The optimal modified reaction time was 4 h, and the strength and modulus of the CNT composite were increased by about 46% and 101%, respectively, compared with the unmodified sample (Fig. 9b).

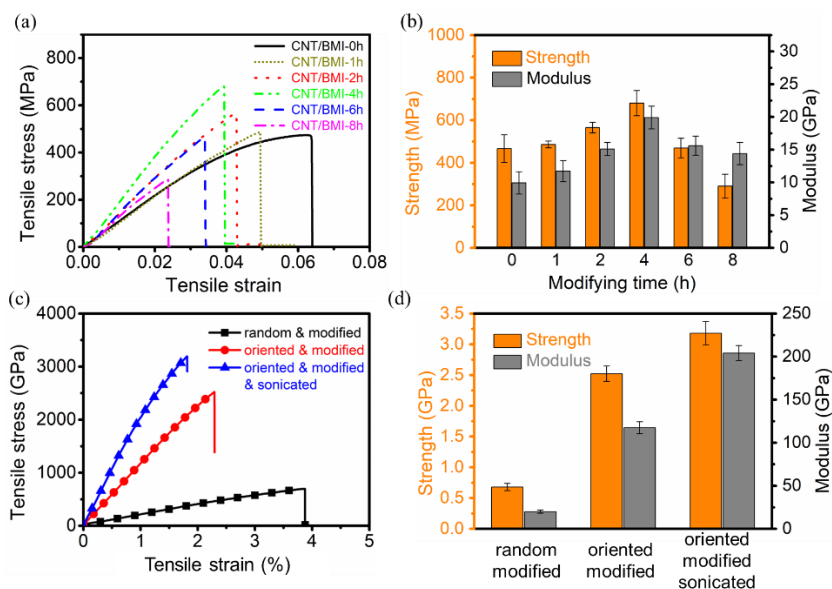


Fig. 9. Mechanical properties of CNT composites under different modification reaction time treatment conditions. (a) stress-strain curves, (b) strength and modulus. Mechanical properties of CNT composites under different treatment conditions. (c) stress-strain curve, (d) strength and modulus.

3.3.3 Effect of ultrasonic cavitation on the modification reaction and properties of CNT composites

In order to further optimize the structure and properties of CNT composites, ultrasonic wave was introduced during the modification reaction of CNT and the influence mechanism of ultrasonic cavitation on the chemical modification reaction and the CNT composites' properties were analyzed. Fig. 9c and d showed the mechanical properties of CNT composites under three treatment conditions

(modified reaction time was 4 h), including random modified CNT composites, oriented modified CNT composites and oriented ultrasonication-assisted modified CNT composites. The experimental results showed that the strength, modulus and toughness of the composites under the three treatment conditions were 0.68 GPa and 19.9 GPa and 14.3 J/cm³, 2.5 GPa and 117.4 GPa and 37.8 J/cm³, 3.2 GPa and 204.0 GPa and 39.2 J/cm³, respectively. It could be seen that the toughness, strength and modulus of oriented CNT composites were improved synchronously by ultrasonication-assisted modification technology. Compared with random modified CNT composites, the strength of oriented modified CNT composites was improved by 257%, while that of oriented ultrasonic assisted modified CNT composites was improved by 357%.

Fig. 10 showed the XPS spectra of CNT films treated with the same modified reaction time (4 h) under the non-ultrasonic conditions and ultrasonic conditions. Obviously, compared with the samples treated without ultrasonication, the C-N peak intensity and area at the position of 285.7eV under ultrasonic conditions were higher, indicating that there were more C-N bonds in the system. Therefore, it was concluded that the introduction of ultrasonic cavitation improved the reaction rate of the chemical modification process of CNT in the system.

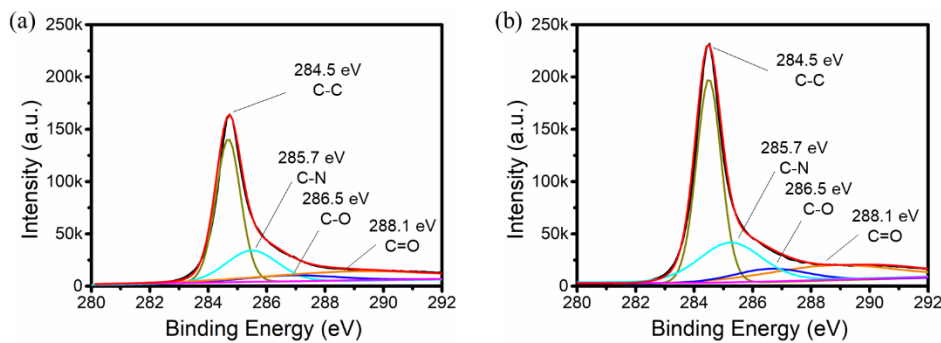


Fig. 10. XPS spectra of modified CNT films (a) with ultrasonication and (b) without ultrasonication.

In summary, the influence mechanism of ultrasonic cavitation on the modification reaction of CNT could be summarized into the following three aspects: ultrasonic cavitation made more CNTs participate in the modification reaction; ultrasonic cavitation increased the number of suspension keys on the surface of CNT, and increased the density of CNT crosslinking and grafting; ultrasonic cavitation improves the reaction rate of CNT modification [15-17].

4 CONCLUSIONS

In this work, the ultrasonic cavitation effect as firstly used to realize the controllable control of CNT bundles' diameter in the composites. On this basis, the ultrasonic cavitation was introduced into the mechanical stretching and chemical modification to achieve high orientation and load transfers of CNT composites. The specific research results are as follows:

1. Ultrasonic cavitation realized the separation of CNT bundles, then the resin molecules diffused into the bundles and prevented their reunion, and the average diameter of bundles was reduced significantly. Ultrasonic cavitation improved the resin distribution uniformity in the composite. The mechanical properties of the composites increased first and then decreased with the increase of ultrasonic energy, and the maximum increase of strength and modulus were 24.8% and 33.9%, respectively.

2. The ultimate stretching ratio of CNT prepreps under the optimal process conditions was increased by 19.3% than that of untreated samples, and the mechanism was attributed to the synergistic effect of ultrasonic induced bundle miniaturization and resin plasticizing. The strength and modulus of aligned CNT nanocomposites treated with a sonication power density of 0.15 W/cm³ were the highest, 2.11 GPa and 104.7 GPa, which were 43.5% and 68.8% higher than those of aligned CNT nanocomposites without ultrasonication.

3. The strength and modulus of the modified CNT film were respectively 46% and 101% higher than that of the unmodified composite material. The strengthening mechanism was that the modified reaction enhanced the interaction between CNTs and the resin infiltration enhanced the interfacial load transfer capacity of the composites. The strength and modulus of ultrasonication-assisted modified oriented CNT

composites were up to 3.2 GPa and 204 GPa, respectively. The influence mechanism of ultrasonic cavitation on the modification reaction was reflected in three aspects: more CNTs participating in the modification reaction, increasing the graft density of single CNT, and increasing the modification reaction rate.

ACKNOWLEDGEMENTS

The authors are grateful to the financial supports from the National Key Research and Development Program of China (2016YFA0203301).

REFERENCES

- [1] Koziol K, Vilatela J, Moiala A, Motta M, Cunniff P, Sennett M, Windle A, High-performance carbon nanotube fiber, *Science*, **318**, 2007, 1892-1895 (doi: [10.1126/science.1147635](https://doi.org/10.1126/science.1147635)).
- [2] Islam MH, Afroj S, Uddin MA, Andreeva DV, Novoselov KS, Karim N, Graphene and CNT-Based Smart Fiber-Reinforced Composites: A Review, *Advanced Functional Materials*, **32**, 2022, 2205723 (doi: [ARTN.2205723.10.1002/adfm.202205723](https://doi.org/ARTN.2205723.10.1002/adfm.202205723)).
- [3] Verma S, Sarma B, Chaturvedi K, Malvi D, Srivastava AK, Emerging graphene and carbon nanotube-based carbon composites as radiations shielding materials for X-rays and gamma rays: a review, *Composite Interfaces*, **30**, 2022, 223-251 (doi: [10.1080/09276440.2022.2094571](https://doi.org/10.1080/09276440.2022.2094571)).
- [4] Coleman JN, Khan U, Blau WJ, Gun'ko YK, Small but strong: A review of the mechanical properties of carbon nanotube-polymer composites, *Carbon*, **44**, 2006, 1624-1652 (doi: [10.1016/j.carbon.2006.02.038](https://doi.org/10.1016/j.carbon.2006.02.038)).
- [5] Chen H, Chen Y, Zhan H, Wu G, Xu JM, Wang JN, Preparation of carbon nanotube/epoxy composite films with high tensile strength and electrical conductivity by impregnation under pressure, *Frontiers of Materials Science*, **13**, 2019, 165-173 (doi: [10.1007/s11706-019-0460-5](https://doi.org/10.1007/s11706-019-0460-5)).
- [6] Jolowsky C, Sweat R, Park JG, Hao A, Liang R, Microstructure evolution and self-assembling of CNT networks during mechanical stretching and mechanical properties of highly aligned CNT composites, *Composites Science and Technology*, **166**, 2018, 125-130 (doi: [10.1016/j.compscitech.2018.04.003](https://doi.org/10.1016/j.compscitech.2018.04.003)).
- [7] Park O-K, Choi H, Jeong H, Jung Y, Yu J, Lee JK, Hwang JY, Kim SM, Jeong Y, Park CR, Endo M, Ku B-C, High-modulus and strength carbon nanotube fibers using molecular cross-linking, *Carbon*, **118**, 2017, 413-421 (doi: [10.1016/j.carbon.2017.03.079](https://doi.org/10.1016/j.carbon.2017.03.079)).
- [8] Suslick KS, The Chemical Effects of Ultrasound, *Scientific American*, **260**, 1989, 80-86 (doi: [10.1038/scientificamerican0289-80](https://doi.org/10.1038/scientificamerican0289-80)).
- [9] Chazot CAC, Hart AJ, Understanding and control of interactions between carbon nanotubes and polymers for manufacturing of high-performance composite materials, *Composites Science and Technology*, **183**, 2019, 107795 (doi: [10.1016/j.compscitech.2019.107795](https://doi.org/10.1016/j.compscitech.2019.107795)).
- [10] Wu G, Chen Y, Zhan H, Chen HT, Lin JH, Wang JN, Wan LQ, Huang FR, Ultrathin and flexible carbon nanotube/polymer composite films with excellent mechanical strength and electromagnetic interference shielding, *Carbon*, **158**, 2020, 472-480 (doi: [10.1016/j.carbon.2019.11.014](https://doi.org/10.1016/j.carbon.2019.11.014)).
- [11] Zhang L, Ma X, Zhang Y, Bradford PD, Zhu YT, Length-dependent carbon nanotube film structures and mechanical properties, *Nanotechnology*, **32**, 2021, (doi: [10.1088/1361-6528/abef92](https://doi.org/10.1088/1361-6528/abef92)).
- [12] Zhang XB, Jiang XR, Qu SX, Zhang H, Yang WG, Lu WB, Effects of ultrasonication on the microstructures and mechanical properties of carbon nanotube films and their based composites, *Composites Science and Technology*, **221**, 2022, 109136 (doi: [10.1016/j.compscitech.2021.109136](https://doi.org/10.1016/j.compscitech.2021.109136)).
- [13] Luo S, Liu T, Wang B, Comparison of ultrasonication and microfluidization for high throughput and large-scale processing of SWCNT dispersions, *Carbon*, **48**, 2010, 2992-2994 (doi: [10.1016/j.carbon.2010.04.006](https://doi.org/10.1016/j.carbon.2010.04.006)).

- [14] Lucas A, Zakri C, Maugey M, Pasquali M, van der Schoot P, Poulin P, Kinetics of Nanotube and Microfiber Scission under Sonication, *Journal of Physical Chemistry C*, **113**, 2009, 20599-20605 (doi: [10.1021/jp906296y](https://doi.org/10.1021/jp906296y)).
- [15] Li Q, Yang H, Coldea TE, Andersen ML, Li W, Zhao H, Enzymolysis kinetics, thermodynamics and structural property of brewer's spent grain protein pretreated with ultrasound, *Food and Bioproducts Processing*, **132**, 2022, 130-140 (doi: [10.1016/j.fbp.2022.01.001](https://doi.org/10.1016/j.fbp.2022.01.001)).
- [16] Zhong X, Huang C, Chen L, Yang Q, Huang Y, Effect of ultrasound on the kinetics of anti-solvent crystallization of sucrose, *Ultrasonics Sonochemistry*, **82**, 2022, 105886 (doi: [10.1016/j.ultsonch.2021.105886](https://doi.org/10.1016/j.ultsonch.2021.105886)).
- [17] Gui Q, Fu L, Hu Y, Di H, Liang M, Wang S, Zhang L, Gold extraction using alternatives to cyanide: Ultrasonic reinforcement and its leaching kinetics, *Minerals Engineering*, **191**, 2023, 107939 (doi: [10.1016/j.mineng.2022.107939](https://doi.org/10.1016/j.mineng.2022.107939)).